4-2020

A Hydrometeorological Assessment of the Historic 2019 Flood of Nebraska, Iowa, and South Dakota

Paul Xavier Flanagan
University of Nebraska-Lincoln, pflanagan@unl.edu

Rezaul Mahmood
University of Nebraska-Lincoln, rmahmood2@unl.edu

Natalie Umphlett
University of Nebraska-Lincoln, numphlett2@unl.edu

Erin M.K. Haacker
University of Nebraska, ehaacker2@unl.edu

Chittaranjan Ray
University of Nebraska-Lincoln, cray@nebraska.edu

A Hydrometeorological Assessment of the Historic 2019 Flood of Nebraska, Iowa, and South Dakota

Authors:

Paul Xavier Flanagan[1,2], Rezaul Mahmood[1,2], Natalie A. Umphlett[1,2], Erin Haacker[3], C. Ray[4], William Sorensen[1,2,] Martha Shulski[2,5], Crystal J. Stiles[1,2,] David Pearson[6], Paul Fajman[6]

Affiliations:

[1]High Plains Regional Climate Center, University of Nebraska-Lincoln, Lincoln, Nebraska, USA

[2]School of Natural Resources, University of Nebraska-Lincoln, Lincoln, Nebraska, USA

[3]Department of Earth and Atmospheric Sciences, University of Nebraska-Lincoln, Lincoln, Nebraska, USA

[4]Nebraska Water Center, University of Nebraska-Lincoln, Lincoln, Nebraska, USA

[5]Nebraska State Climate Office, University of Nebraska-Lincoln, Lincoln, Nebraska, USA

[6]The National Weather Service, Omaha, Nebraska, USA

Corresponding author address: Paul Flanagan, High Plains Regional Climate Center, School of Natural Resources, 701 Hardin Hall South, 3310 Holdrege Street, Lincoln, NE, 68583. Email: pflanagan3@unl.edu; Phone: 402-472-6706

Early Online Release: This preliminary version has been accepted for publication in *Bulletin of the American Meteorological Society*, may be fully cited, and has been assigned DOI 10.1175/BAMS-D-19-0101.1. The final typeset copyedited article will replace the EOR at the above DOI when it is published.

Abstract

During early 2019, a series of events set the stage for devastating floods in eastern Nebraska, western Iowa, and southeastern South Dakota. When the floodwaters hit, dams and levees failed, cutting off towns, while destroying roads, bridges, and rail lines, further exacerbating the crisis. Lives were lost and thousands of cattle were stranded. Estimates indicate that the cost of the flooding has topped $3 billion as of August 2019, with this number expected to rise.

After a warm and wet start to winter, eastern Nebraska, western Iowa, and southeastern South Dakota endured anomalously low temperatures and record-breaking snowfall. By March 2019, rivers were frozen, frost depths were 60-90 cm, and the water equivalent of the snowpack was 30-100 mm. With these conditions in place, a record-breaking surface cyclone rapidly developed in Colorado and propagated eastward, producing heavy rain towards the east and blizzard conditions toward the west. In areas of eastern Nebraska, western Iowa, and southeastern South Dakota, rapid melting of the snowpack due to this rain-on-snow event quickly led to excessive runoff that overwhelmed rivers and streams. These conditions brought the region to a standstill.

In this paper, we will provide an analysis of the antecedent conditions in eastern Nebraska, western Iowa and southeastern South Dakota, the development of the surface cyclone that triggered the historic flooding, along with a look into the forecast and communication of flood impacts prior to the flood. The study used multiple datasets, including in-situ observations and reanalysis data. Understanding the events that led to the flooding could aid in future forecasting efforts.

Accepted for publication in *Bulletin of the American Meteorological Society.* DOI 10.1175/BAMS-D-19-0101.1.

Introduction

During the late winter season of 2019, a combination of anomalous events led to devastating floods across the central United States (U.S.; Fig. 1). These events were punctuated by the passage of an extraordinarily deep surface cyclone that propagated across the region on 12-14 March. This storm system produced extreme weather, including blizzard conditions stretching from Colorado and Kansas through the Dakotas, and widespread liquid precipitation events in areas just to the east. Numerous daily precipitation records were broken, with some locations setting new records for highest one-day precipitation for the month of March. Low pressure records over Colorado and Kansas were also broken. This flood event was exacerbated by the surface conditions across eastern Nebraska, western Iowa, and southeastern South Dakota (hereafter referred to as the study area), namely the widespread frozen or saturated soils, frozen rivers, and above average river streamflow conditions (Fig. 2a) that led to numerous record river crests across the region (Fig. 2b, 2c, 2d, 9c). Initially, the excessive runoff overwhelmed smaller tributary rivers in study area, which flow to larger rivers in the Platte and Missouri River basins. This resulted in failed levees and dams, leaving downriver locations overwhelmed with significant ice jams and water flow. This set of circumstances led to one of the most catastrophic flood events documented across the study area. Prior to the event, National Weather Service (NWS) offices were forecasting and communicating the possibility of record-breaking floods across the study area. Ultimately, the Federal Emergency Management Agency (FEMA) declared a major disaster for both Nebraska and Iowa, with a preliminary damage estimate of at least $3 billion.

Accepted for publication in *Bulletin of the American Meteorological Society.* DOI 10.1175/BAMS-D-19-0101.1.

No single factor can explain the occurrence of this historic flood event. Hence, it is critical to understand how the combination of meteorological, climatological, and hydrological conditions led to large-scale flooding across the region. The purpose of this brief paper is to 1) discuss the rapid cyclogenesis event and preceding surface and hydrological conditions across eastern Nebraska, western Iowa, and southeastern South Dakota, 2) examine how the synergy between these independent factors led to large-scale major flooding, and 3) investigate the forecast and communication of flood impacts across Nebraska, Iowa, and South Dakota.

Prior Hydrometeorological Context

During the 2018 fall (Fig. 3a) and 2018/2019 winter (Fig. 3b) seasons, sea surface temperatures (SST) across the tropical Pacific were warmer than normal, (Fig. 3) indicating a developing El Niño event. These SST conditions increased the chances of a wetter winter season across the southern U.S., near normal moisture conditions in the study area, and a milder winter season across the northern U.S., including most of the study area (Climate Prediction Center 2017). Additionally, the North Atlantic Oscillation (NAO) was positive during December and January (0.61 and 0.59), the Arctic Oscillation (AO) was weakly positive (December; 0.110) and negative (January; -0.713), and the Pacific-North American (PNA) teleconnection pattern was positive (0.86 and 0.83) (available at https://www.cpc.ncep.noaa.gov/products/precip/CWlink/pna/nao.shtml, https://www.cpc.ncep.noaa.gov/products/precip/CWlink/daily_ao_index/ao.shtml, and https://www.cpc.ncep.noaa.gov/products/precip/CWlink/pna/norm.pna.monthly.b5001.current.ascii.table, respectively). It is well known that the positive NAO would force slightly

Accepted for publication in *Bulletin of the American Meteorological Society.* DOI 10.1175/BAMS-D-19-0101.1.

warmer temperatures over the central U.S. with little impact on precipitation (Hurrell et al. 2003), the weak AO would not largely impact the overall weather (Wang et al. 2005), and the positive PNA would drive warmer temperatures over the western and north central U.S. (Leathers et al. 1991). The early part of the winter season (December 2018 and January 2019) was warmer and wetter relative to February and March in the study area (Fig. 4). Runoff from river systems were above average across most of the region (Fig. 2a) prior to freezing. Precipitation across the region was above normal (Fig. 4c), with average snowfall totals through the end of January at approximately 30.5 cm. Even so, because of the warmer early winter season temperatures (Fig. 4a), no significant snowpack had developed by the end of January. Part of the moisture from the early winter season precipitation (either rain or snow) was absorbed by the land surface and as a result, soils were nearly saturated during this portion of 2019 (Fig. 2e). In January, temperatures across the study area had begun to decrease such that the soils were frozen by the end of the month.

It was also found that the center of the warm SST anomalies in the Pacific had shifted from the early to late winter. The primary center was now seen in the central tropical Pacific (Fig. 3b). This location of warm SST anomalies has been linked to increased chances of excessive precipitation over the south-central U.S. (Livezey et al. 1997; Flanagan et al. 2019). Further, these central Pacific warm SST anomalies are not associated with the typical higher chance of northern U.S. warming, seen during typical eastern tropical Pacific warm events (Ashok et al. 2007). The NAO continued to be positive during February and March (0.29 and 1.23), the AO became strongly positive (1.149 and 2.116), and the PNA shifted to negative (-1.08 and 0.25), with the month of March showing a positive PNA index owing to large (~ 0.5 to 1.3) positive daily PNA values after the

Accepted for publication in *Bulletin of the American Meteorological Society.* DOI 10.1175/BAMS-D-19-0101.1.

cyclogenesis event. This is an interesting feature, as both positive NAO and AO would normally aid in keeping temperatures milder during the winter season over the central U.S. As indicated above, this was not the case. The colder temperatures during February and March were caused by a persistent northwesterly flow regime over the northwestern and north central U.S. due to ridging across the northwestern U.S. The negative PNA regime can force such a pattern over this portion of the U.S. (Leathers et al. 1991). Thus, the cold temperatures were linked to the persistent negative PNA signal during this portion of winter 2019. Frigid temperatures occurred across the region from late January through March (Fig. 4b). This shift in temperatures finally caused rivers to freeze, with the Platte River having an ice depth around 43 cm (at Leshara, Nebraska). Further, with wet soils and lacking an insulating snowpack, the cold temperatures formed a deep and hard frost layer prior to March (Fig. 5a). With these cooler temperatures came a changeover of precipitation, as snowfall began to occur more frequently. The above average precipitation resulted in numerous snowfall records being broken across the region (Fig. 4c, 4d), setting up a deep and moist snowpack (Fig. 5b, 5d). Approximately 10-20 cm of snow was observed across the region (Fig 5b), with the snowpack showing around 3-10 cm of snow water equivalent (SWE) (Fig. 5d). The frozen soil did not allow for infiltration of moisture from melted snow and expected that a rapid melting would spell disaster for the region.

The Global Historical Climatology Network stations that show the season's top-5 snowfall records for 2018-2019 are highlighted in figures 4c and 4d. It is to be noted that other stations within the region had 'records' but did not pass the quality control checks we utilized to produce the station plots. In previous spring flood events, namely 1881 and 1952, hydrometeorological conditions were similar to conditions of 2019. For the 1881

Accepted for publication in *Bulletin of the American Meteorological Society.* DOI 10.1175/BAMS-D-19-0101.1.

floods, 60-80 cm of river ice was reported and for the 1952 event, SWE values were around 8-13 cm along with saturated soils from wetter than average fall and winter seasons (Department of Commerce, Hydrologic Services Division 1954). Overall, the region was setup for a flood near or above the previous floods of record in the region. Early winter hydrological conditions, extreme cold and anomalous precipitation during the later winter put in place conditions ready for a rapid, significant flood event for the study region.

Rapid Cyclogenesis of March 12-14, 2019

Reanalysis data from the National Centers for Environmental Prediction/National Center for Atmospheric Research (NCEP/NCAR) Reanalysis version 1 (Kalnay et al. 1996) were utilized to provide a synoptic overview of the event. The dataset is available from the Earth System Research Laboratory (ESRL) Physical Science Division (PSD) database (https://www.esrl.noaa.gov/psd/data/gridded). This 2.5° x 2.5° globally gridded dataset is updated daily, from 1948 to present. Using this dataset, we analyzed sea level pressure (SLP); surface temperature and winds; precipitable water; 250 and 500 hPa winds and geopotential heights; and 850 and 925 hPa winds, temperature, and heights using the NCAR Command Language (NCL; http://dx.doi.org/10.5065/D6WD3XH5). This dataset was utilized to derive all advection terms. Standardized anomalies were created for temperature, geopotential height, precipitable water, and SLP to present critical variables in the context of the time of year and regional climate. This was accomplished by using 21-day centered means from a 30-year base period (1981-2010) and standardized by the standard deviation, given by

Accepted for publication in *Bulletin of the American Meteorological Society.* DOI 10.1175/BAMS-D-19-0101.1.

158 $$\sigma_A = \frac{X - \mu}{\sigma}$$

159 where X is the observed grid-point value, μ is the centered 21-day climatological mean,
160 and σ is the standard deviation (Durkee et al. 2012).

161 On 12-13 March, a rapid surface cyclogenesis event took place across the central
162 U.S. (Fig. 6). A closed trough across the southwestern U.S. propagated towards the north
163 at the same time as a long-wave trough shifted down from the north. These two systems
164 began interacting late on 12 March, in the lee of the Rocky Mountains in eastern Colorado.
165 As this area already had a low-pressure zone near the surface (Fig. 6a), and owing to the
166 converging troughs across the region (Fig. 6c, 6d), a rapid lee cyclogenesis event took place
167 (Fig. 6b). This caused surface pressure values to plummet, leading to a record-low pressure
168 reading over eastern Colorado (970.4 hPa; NWS Cheyenne WY 2019; Colorado Climate
169 Center 2019) and Kansas (974.7 mb; NWS Dodge City, KS 2019), with a drop of 24 hPa
170 (from 994 hPa to 970 hPa) in 15 hours on 12 March (NWS Hastings NE 2019). This rapid
171 lee cyclogenesis event was the primary driver of the excessive precipitation which occurred
172 over the study region on 13 March.

173 However, prior to this cyclogenesis event, the gradient zone between the upper
174 level closed trough and the broad ridge over the eastern U.S. (Fig. 6c) caused southerly
175 flow across a majority of the central U.S. (Fig. 7a). This caused warm, moist air to begin
176 to advect over the central part of the country (Fig. 7b). As the cyclogenesis event began to
177 take place, the advection regime strengthened, bringing an anomalously warm (Fig. 7c)
178 and near record breaking deep moist airmass over the central U.S. (Fig. 7d). This is
179 reflected in the record precipitable water values across the region, with atmospheric

Accepted for publication in *Bulletin of the American Meteorological Society.* DOI 10.1175/BAMS-D-19-0101.1.

soundings at Omaha, NE (2.44 cm) and North Platte, NE (1.80 cm) breaking their 13 March 0000 UTC records (2.159 and 1.37 cm, respectively) and Topeka, KS (2.57 cm) nearly breaking its record (2.62 cm) at 12 March 1200 UTC. Note that all of these soundings were taken prior to precipitation in their area. The advection of warm air resulted in rapid snow melt that reduced the snowpack from a peak depth of 10-30 cm on 9 March to a trace on 15 March across most of eastern Nebraska and western Iowa (Fig. 5b, 5c). While temperatures were not high enough to cause large scale snowmelt in southeastern South Dakota (Fig. 5b, 5c), temperatures were warm enough for the precipitation to fall as rain instead of snow (NWS Sioux Falls SD 2019). This can further be seen in the SWE figures (Fig. 5d, 5e), which show a rapid decrease across most of Nebraska and Iowa, while only extreme southeastern South Dakota saw a large decrease in snow coverage and the remainder of South Dakota maintained its snowpack. Thus, when rainfall began later on 12 March, runoff from prior snowmelt was already flowing into the region's streams and rivers. The excessive precipitation forced by the cyclone quickly caused rivers to rise to record-setting levels, overwhelming regional water storage infrastructure (Fig. 2b).

Flood Forecast Discussion

Prior to the event, the Weather Prediction Center (WPC) forecasting approximately 50-75 mm in their 72-hour Quantitative Precipitation Forecast (QPF) from 0000 UTC 12 March to 0000 UTC 15 March (Fig. 8). The system was expected to efficiently produce precipitation from the anomalously moist air mass that was being advected into the area as the lee cyclone rapidly developed and propagated to the northeast.

Accepted for publication in *Bulletin of the American Meteorological Society.* DOI 10.1175/BAMS-D-19-0101.1.

Weeks prior to the flooding event, NWS Omaha/Valley officials were in communication with regional officials (emergency managers, Nebraska Emergency Management Agency (NEMA), etc.) and local media regarding the risk of flooding because of the extensive ice coverage of regional rivers. There were weekly ice jam update conference calls with core NWS Omaha/Valley partners and local media. The latter relayed flood potential and rainfall forecast information to stakeholders and local and state officials in the weeks leading up to the flood event. These conference calls disseminated the probabilistic risk of spring flood events, using information such as current streamflow percentiles, river ice status, snowpack depth, etc. As 12 March drew closer, clarity into the extreme nature of the event increased. A week prior to the flood event, NWS Omaha/Valley sent out an updated spring flood outlook, which highlighted an increased threat for major flooding owing to the anomalous hydrological conditions throughout the area. When the model output precipitation forecast for 12 March to 14 March started to take focus, local NWS offices began issuing flood watches for the region. Subsequently, these watches were updated to reflect the expected record-breaking nature of the event on the morning of 12 March over a large section of the NWS Omaha/Valley forecast area. These forecasts were supported by numerous observational (e.g., streamflow, river ice and snowpack) and modeling resources (e.g., GEFS, ECMWF) including the ensemble situational awareness table (ESAT) which showed the potential for an extreme event a week prior to the flood event.

The first round of precipitation came in the late afternoon on 12 March, but did not produce large-scale precipitation across the region as the forcing for ascent was weak at this time. Later, on 12-13 March, multiple rounds of precipitation came through the study

Accepted for publication in *Bulletin of the American Meteorological Society.* DOI 10.1175/BAMS-D-19-0101.1.

area, as forecasted. Most areas in eastern Nebraska and western Iowa received around 12-25 mm of liquid precipitation with isolated areas reporting around 25-50 mm (Fig. 9a). However, areas farther west, mainly in the tributary region of the Platte River (e.g. the Loup and Wood Rivers) and in southeastern South Dakota, received 40-75 mm of primarily liquid precipitation on 12-14 March. Thus, the storm total precipitation amounts matched well with the WPC forecasted precipitation totals. At approximately 1400 UTC 14 March, precipitation began to cease in the study region due to a rapidly developing area of dry air forced by the occlusion process of the surface low. Farther west in Nebraska and South Dakota, snowfall began or continued to fall on the cold side of the occluding cyclone, causing blizzard conditions and producing around 15 cm of snow across most of the western portions of Nebraska and South Dakota (Fig. 9b). This snow would later melt and further exacerbate flood conditions across the region. Due to the existing snowpack and frozen soil conditions, almost all of this precipitation quickly ran into rivers and creeks. The large amount of water produced by the melting snow (Fig. 9c) and the excessive runoff from the liquid precipitation quickly overwhelmed the watersheds across the region and verified the NWS flood warnings.

Summary and Perspective

During mid-March of 2019, the study area was impacted by record-setting floods. This flood event was triggered by precipitation forced by the record-low surface cyclone that rapidly developed across eastern Colorado and brought record daily precipitation amounts across portions of Nebraska, either through rain or the heavy snowfall. Preceding the flood event, weeks of anomalously low surface temperatures and accumulation of snow

Accepted for publication in *Bulletin of the American Meteorological Society.* DOI 10.1175/BAMS-D-19-0101.1.

prior to the cyclogenesis event caused soil conditions that led to anomalously high runoff. In addition, warm advection and rainfall quickly melted the abnormally thick snowpack that blanketed most of the study region. Although the rapid cyclogenesis of the lee cyclone in eastern Colorado is typical for this time of the year (Petterssen 1956; Chung et al. 1976; Roebber 1984; Pierrehumbert 1986; Clark 1990; Schultz and Doswell 2000), this particular event produced a surface cyclone that was more intense than any previously recorded in the Colorado and Kansas. Together, the record deep low-pressure system and the anomalously moist air mass brought about 12-25 mm of precipitation over southeastern Nebraska and southwestern Iowa, 25-50 mm across northeastern Nebraska and northwestern Iowa, and 40-75 mm over large portions of central Nebraska and southern South Dakota. With the rapidly melting, moist snow pack and ice jams on the waterways, the precipitation quickly exceeded the channel flow capacity of rivers in the region and began the expansive flooding.

While not a focus of the research presented here, the authors believe the extensive and costly event highlights the current forecasting ability of the WPC QPF capabilities. Their forecasts weeks and days ahead of the primary and catastrophic flood event across the study region provided much-needed warning far enough ahead of time that it likely saved numerous lives and personal property. This was aided by the probabilistic and deterministic forecasts which showed the heightened risk for an extreme weather event and subsequent flood a week before the cyclogenesis event occurred. Further, this successful forecast highlights the importance of extensive, high spatial resolution monitoring networks. Without the knowledge of the frozen soils and large snowpack across the region, local NWS offices would have lacked crucial information into the scale and magnitude of

Accepted for publication in *Bulletin of the American Meteorological Society.* DOI 10.1175/BAMS-D-19-0101.1.

the flood event that took place. Further, this event established far above normal hydrological conditions throughout the study region, i.e., the Missouri River Basin. After the flood event in March, meteorological and hydrological conditions have been such that the region is still completely saturated heading into the 2019-2020 winter season, meaning that river levels are largely above normal and soil moisture levels are at or near capacity. Further, owing to the above average water conditions throughout the Missouri River Basin, heavy precipitation events throughout 2019 caused rapid flood events, especially in southeastern South Dakota. It would be remiss not to note that the flood event of March 2019 helped to developed extreme hydrologic conditions across Nebraska, Iowa and South Dakota which are conducive for further flood events in 2020. Lastly, this event underscored the importance of communication between forecasters and local/regional stakeholders, local officials and the media. This allowed NWS officials to disseminate crucial flood forecast information to "key players" rather than using the time prior to the event searching for "the right people to talk to."

Acknowledgements

NCEP/NCAR reanalysis data was taken from the NOAA-ESRL Physical Sciences Division, Boulder Colorado from their Web site at https://www.esrl.noaa.gov/psd/data/gridded. CPC Global Unified Precipitation data provided by the NOAA/OAR/ESRL PSD, Boulder, Colorado, USA, from their Web site at https://www.esrl.noaa.gov/psd/. We would like to thank NCAR for the NCAR Command Language (Version 6.2.1) [Software]. (2014). Boulder, Colorado: UCAR/NCAR/CISL/TDD. http://dx.doi.org/10.5065/D6WD3XH.

Accepted for publication in *Bulletin of the American Meteorological Society.* DOI 10.1175/BAMS-D-19-0101.1.

References

American Meteorological Society, 2019: Lee Cyclogenesis. Accessed 29 July 2019, http://glossary.ametsoc.org/wiki/Lee_cyclogenesis

American Meteorological Society, cited 2019: "Lee Cyclogenesis". Glossary of Meteorology. [Available online at http://glossary.ametsoc.org/wiki/Lee_cyclogenesis]

Ashok, K., S. K. Behera, S. A. Rao, H. Weng, and T. Yamagata, 2007: El Niño Modoki and its possible teleconnection. *J. Geophys. Res.*, **112,** C11007. doi:10.1029/2006JC003798.

Chung, Y-S, K. D. Hage and E. R. Reinelt, 1976: On lee cyclogenesis and airflow in the Canadian Rocky Mountains and the East Asian mountains, *Mon. Wea. Rev*., **104**, 879–891.

Clark, J. H. E., 1990: An observational and theoretical study of Colorado lee cyclogenesis. *J. Atmos. Sci*., **47,**1541–1561.

Colorado Climate Center, 2019: Storm Records. Accessed 9 December 2019, https://climate.colostate.edu/pdfs/storm_records.pdf

CPC, 2017: El Niño and La Niña – related winter features over North America. Accessed 22 August 2019, https://www.cpc.ncep.noaa.gov/products/analysis_monitoring/ensocycle/nawinter.shtml

Accepted for publication in *Bulletin of the American Meteorological Society.* DOI 10.1175/BAMS-D-19-0101.1.

315 Department of Commerce, Hydrologic Services Division, 1954: Floods of 1952 Upper
316 Mississippi – Missouri – Red River of the North. *Technical Report 23,* 101 pp,
317 https://www.nws.noaa.gov/oh/hdsc/Technical_papers/TP23.pdf

318 Durkee, J. D., L. Campbell, K. Berry, D. Jordan, G. Goodrich, R. Mahmood,
319 and S. Foster, 2012: A synoptic perspective of the record 1–2 May 2010 mid-South
320 heavy precipitation event. *Bull. Amer. Meteor. Soc.*, **93**, 611–620.

321 Flanagan, P. X., J. B. Basara, J. C. Furtado, E. R. Martin, X. Xiao, 2019: Role of sea surface
322 temperatures in forcing circulation anomalies driving United States Great Plains
323 pluvial years. *J. Climate*, EOR, doi: https://doi.org/10.1175/JCLI-D-18-0726.1

324 Hurrell, J. W., Y. Kushnir, G. Ottersen, and M. Visbeck, 2003: *The North Atlantic*
325 *Oscillation: Climate Significance and Environmental Impact. Geophys.*
326 *Monogr.*, Vol. 134, Amer. Geophys. Union, 279 pp.

327 Kalnay, E., and Coauthors, 1996: The NCEP/NCAR 40-Year Reanalysis Project. *Bull.*
328 *Amer. Meteor. Soc.*, **77**, 437–471.

329 Leathers, D. J., B. Yarnal, and M. A. Palecki, 1991: The Pacific/North American
330 teleconnection pattern and United States climate. Part I: Regional temperature and
331 precipitation associations. *J. Climate*, **4,** 517–528.

332 Livezey, R. E., M. Masutani, A. Leetmaa, H. Rui, M. Ji, and A. Kumar, 1997: 882
333 Teleconnective response of the Pacific–North American region atmosphere to 883
334 large central equatorial Pacific SST anomalies. *J. Climate*, **10**, 1787–1820, 884
335 https://doi.org/10.1175/1520-0442(1997)0102.0.CO;2.

Accepted for publication in *Bulletin of the American Meteorological Society.* DOI 10.1175/BAMS-D-19-0101.1.

Nebraska Emergency Management Agency, 2019: News release, By the numbers – Nebraska's historic floods. https://nema.nebraska.gov/sites/nema.nebraska.gov/files/press/doc/NEMA%20AM%20NewRelease%203.17.19.pdf.

National Weather Service Cheyenne, Wyoming Office, 2019: March 13th and 14th, 2019 Bomb Blizzard, Accessed 29 July 2019, https://www.weather.gov/cys/March13142019Blizzard

National Weather Service Hastings, Nebraska Office, 2019: Mid-March 2019: Historical, Catastrophic Flooding Impacts Parts of Central/South Central Nebraska, Accessed 29 July 2019, https://www.weather.gov/gid/march2019flood

National Weather Service Sioux Falls, South Dakota Office, 2019: Heavy Rain and Snow Melt Create Widespread Flooding – March 13-14, 2019, Accessed 15 November 2019, https://www.weather.gov/fsd/20190314-Flooding

National Weather Service Dodge City, Kansas Office, 2019: Historic low pressure system affects the Plains!, Accessed 9 December 2019, https://www.weather.gov/ict/event_20190313

Petterssen, S., 1956: *Weather Analysis and Forecasting. Volume I: Motion and Motion Systems*. McGraw-Hill, 428 pp.

Pierrehumbert, R. T., 1986: Lee cyclogenesis. *Mesoscale Meteorology and Forecasting,* P. S. Ray, Ed., Amer. Meteor. Soc., 493–515.

Accepted for publication in *Bulletin of the American Meteorological Society.* DOI 10.1175/BAMS-D-19-0101.1.

356 Roebber, P. J., 1984: Statistical analysis and updated climatology of explosive cyclones,
357 *Mon. Wea. Rev.*, **112**, 1577–1589.

358 Schultz, D. M., and C. A. Doswell III, 2000: Analyzing and forecasting Rocky Mountain
359 lee cyclogenesis often associated with strong winds. *Wea. Forecasting,* **15,** 152–
360 173.

361 Wang, D., C. Wang, X. Yang, and J. Lu, 2005: Winter Northern Hemisphere surface air
362 temperature variability associated with the Arctic Oscillation and North Atlantic
363 Oscillation. *J. Geophy. Res. Lett.*, **32**, L16706,
364 doi:https://doi.org/10.1029/2005GL022952.

365

Accepted for publication in *Bulletin of the American Meteorological Society.* DOI 10.1175/BAMS-D-19-0101.1.

Figure Captions

Figure 1: European Space Agency (ESA) (a) Sentinel-2A Level-1C visible band satellite image on 16 March 2019. Panel (b) Sentinel-2A Level-1C visible band satellite image on 10 January 2019. Also included is a zoomed-out image from 16 March 2019 showing the location of the zoomed in area for (a) and (b). Sentinel-2 images taken from https://apps.sentinel-hub.com/eo-browser/?lat=40.2685&lng=-95.6738&zoom=10&time=2019-03-16&preset=1_TRUE_COLOR&datasource=Sentinel-2%20L2A. The upper red dot in (a) represents the approximate location of the river gauge (Fig. 2c) in Turin, Iowa and the lower red dot in (a) represents the approximate location of the river gauge (Fig. 2d) in Nebraska City, NE.

Figure 2: United States Geological Survey (USGS) United States real-time streamflow for (a) November 12th 2019 and (b) March 16th 2019. The streamflow measurements are in percentiles based on the entire record of each station. Stations with under 30 years of coverage are not used. USGS gauge height (in feet) readings on the (c) Little Sioux River near Turin, IA and (d) Missouri River near Nebraska City from 1 November 2018 to 31 March 2019. USGS gauge data available at https://waterdata.usgs.gov/nwis/rt. Panel (e) are the Climate Prediction Center Leaky Bucket Model modeled soil moisture percentiles for January 2019.

Figure 3: National Oceanic and Atmospheric Association Optimum Interpolation Sea Surface Temperature (SST) V2 anomalies for (a) September, October and November 2018

Accepted for publication in *Bulletin of the American Meteorological Society.* DOI 10.1175/BAMS-D-19-0101.1.

and (b) December 2018, January, and February 2019 in °C. Anomalies were calculated using the 1981-2010 base period climatology.

Figure 4: Global Historical Climatology Network (GHCN) station (a) monthly surface daily temperature anomalies for December and January °C, (b) monthly surface daily average temperature anomalies for February and March 2019 in °C, (c) monthly precipitation percent of normal for December 2018 and January 2019, (d) monthly precipitation percent of normal for February and March 2019. Stations were filtered by length of record, with only stations having at least 50 years of data prior to 2019 being accepted into the analysis. Anomalies were calculated using the period of record for each station. Daily temperature averages were computed as an average between the maximum and minimum daily temperature averages for each month. Station 2018-2019 snow season snowfall total records include a red symbol, with a circle representing a new record, a star is for a 2nd highest snowfall observation, 3 lines for a 3rd highest snowfall observation, 2 lines for a 4th highest snowfall observation, and a triangle for a 5th highest snowfall observation.

Figure 5: (a) Automated Weather Data Network (AWDN) 7-day soil temperature (°C) observations for 6 March to 12 March. National Operational Hydrologic Remote Sensing Center (NOHRSC) modeled (b) snow depth in cm for 9 March 2019 (c) 15 March and (d) snow water equivalent in cm for 9 March 2019 and (e) 15 March. Available at https://www.nohrsc.noaa.gov/.

Accepted for publication in *Bulletin of the American Meteorological Society.* DOI 10.1175/BAMS-D-19-0101.1.

Figure 6: NCEP/NCAR Reanalysis daily averaged data for 12 March. Panel (a) is the daily averaged 500 sea level pressure (contoured) and the standardized anomaly (color filled) for March 12th. Geopotential height contours go from 900 to 1050 by 10 mb and the standardized anomalies are color filled from -8 to 8 by 1. Panel (b) is the daily averaged 500 sea level pressure (contoured) for March 13th. The contours for (b) are the same as (a). Panel (c) is the daily averaged 500 hPa geopotential height (contoured) and the standardized anomaly (color filled) for March 12th. Geopotential height contours from 5300 to 5700 with 60 m interval and the standardized anomalies are color filled from -6 to 6 by 1. Panel (d) is the daily averaged 500 hPa geopotential height (contoured) and the standardized anomaly (color filled) for March 13th. The contours for (d) are the same as (c).

Figure 7: NCEP/NCAR Reanalysis (a) 925 mb *v* wind standardized anomalies. Panel (b) are the reanalysis 925 moisture advection standardized anomalies (g kg^{-1} s^{-1}), specific humidity standardized anomalies (g kg^{-1} contoured from -12 to 12 by 2) and standardized anomaly vector wind. Panel (c) is the surface (1000 hPa) temperature standardized anomalies (°C). Panel (d) is the precipitable water standardized anomalies (kg m^{-2}). Anomalies are from the two-day period of 12 March through 13 March 2019.

Figure 8: WPC QPF forecast made on 11 March for the 72-hour period beginning on 12 March at 0000 UTC and ending on 15 March at 0000 UTC.

Accepted for publication in *Bulletin of the American Meteorological Society.* DOI 10.1175/BAMS-D-19-0101.1.

Figure 9: Panel (a) Composite radar mosaic for March 13th 2019 at 0855 UTC from the UCAR Warm Season Precipitation Episodes image archive available at http://www2.mmm.ucar.edu/imagearchive/. Panel (b) Composite radar mosaic for March 13th 2019 at 1555 UTC from the UCAR Warm Season Precipitation Episodes image archive. Panel (c) CPC Global Unified Gauge-based daily precipitation analysis for 12-14 March. Precipitation is in mm. Panel (d) is the accumulated snow for 12-15 March 2019 in inches. Available at https://www.weather.gov/fsd/20190314-Flooding.

Accepted for publication in *Bulletin of the American Meteorological Society.* DOI 10.1175/BAMS-D-19-0101.1.

462 **Figures**

463

464

(a)

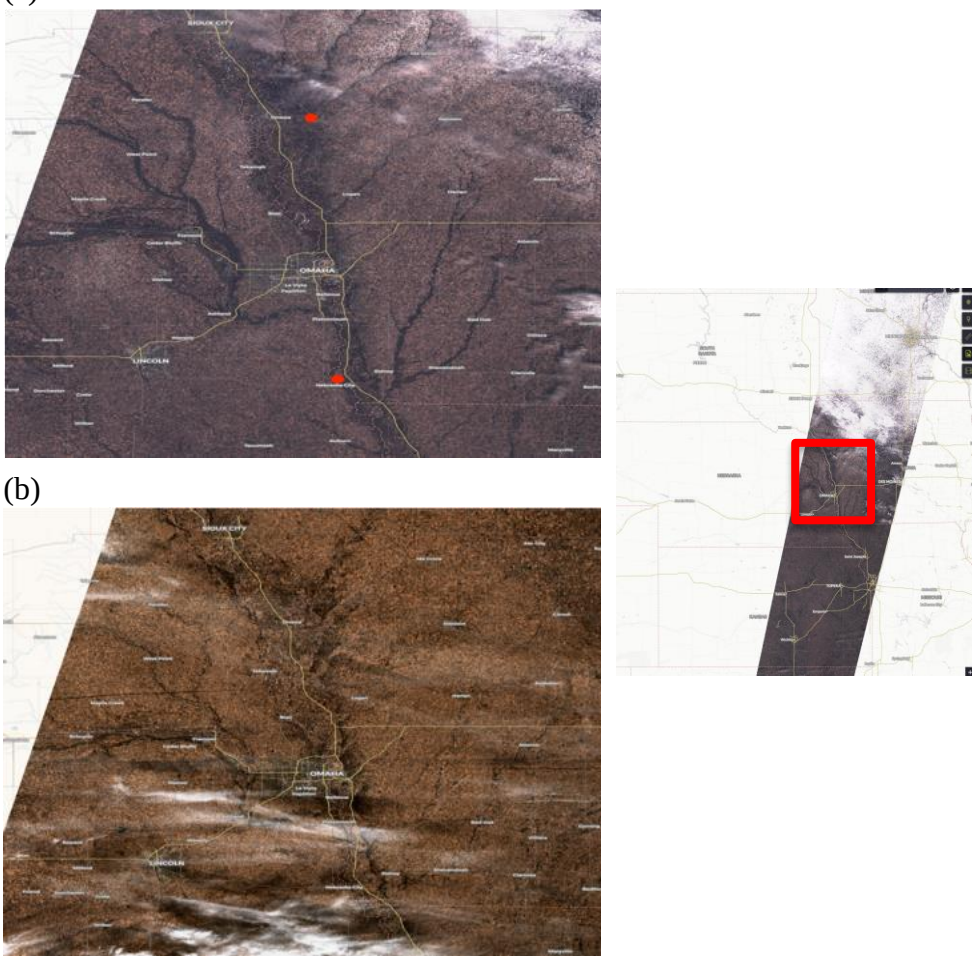

(b)

Figure 1: European Space Agency (ESA) (a) Sentinel-2A Level-1C visible band satellite image on 16 March 2019. Panel (b) Sentinel-2A Level-1C visible band satellite image on 10 January 2019. Also included is a zoomed-out image from 16 March 2019 showing the location of the zoomed in area for (a) and (b). Sentinel-2 images taken from https://apps.sentinel-hub.com/eo-browser/?lat=40.2685&lng=-95.6738&zoom=10&time=2019-03-16&preset=1_TRUE_COLOR&datasource=Sentinel-2%20L2A. The upper red dot in (a) represents the approximate location of the river gauge (Fig. 2c) in Turin, Iowa and the lower red dot in (a) represents the approximate location of the river gauge (Fig. 2d) in Nebraska City, NE.

465

Accepted for publication in *Bulletin of the American Meteorological Society.* DOI 10.1175/BAMS-D-19-0101.1.

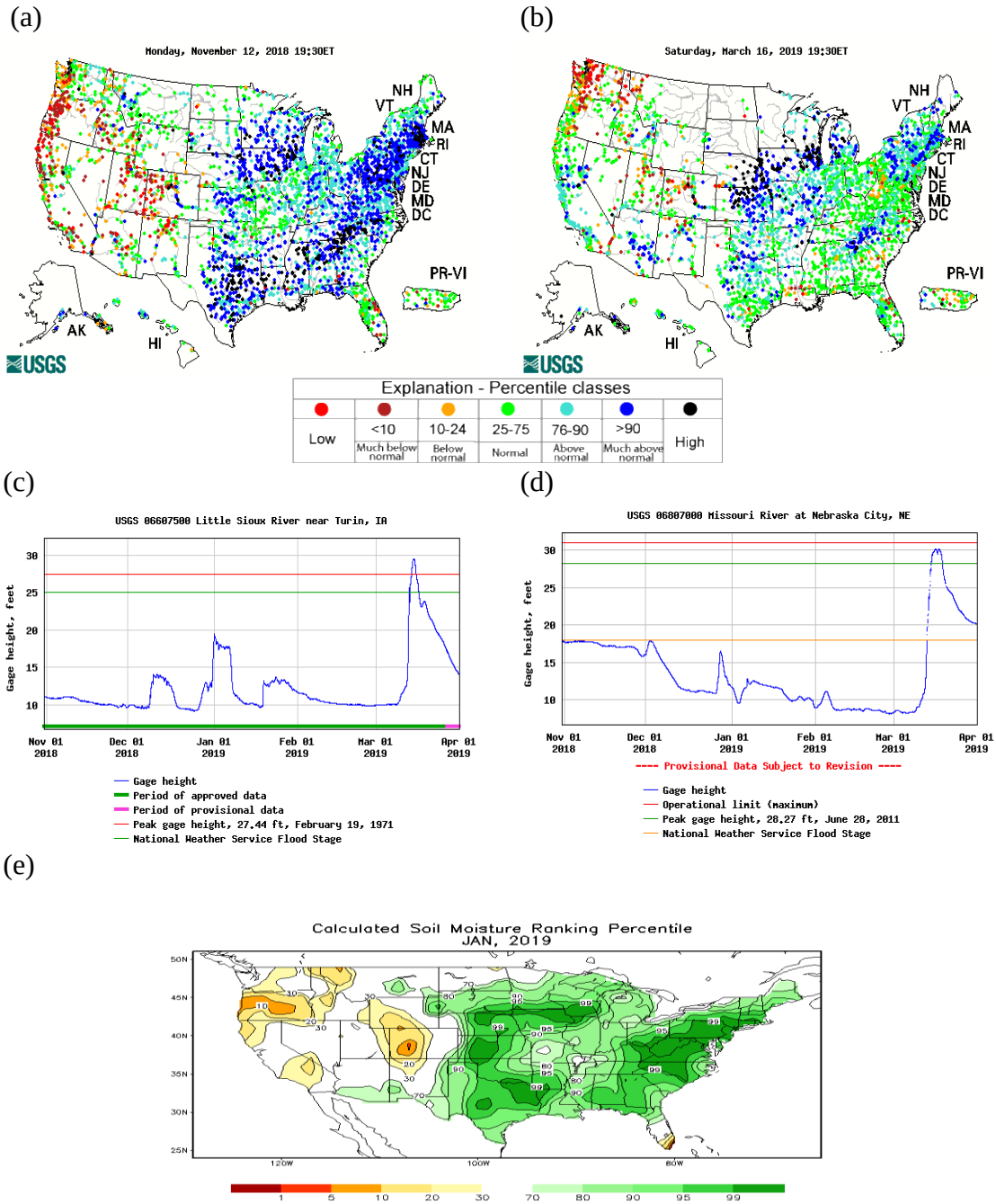

Figure 2: United States Geological Survey (USGS) United States real-time streamflow for (a) November 12th 2019 and (b) March 16th 2019. The streamflow measurements are in percentiles based on the entire record of each station. Stations with under 30 years of coverage are not used. USGS gauge height (in feet) readings on the (c) Little Sioux River near Turin, IA and (d) Missouri River near Nebraska City from 1 November 2018 to 31 March 2019. USGS gauge data available at https://waterdata.usgs.gov/nwis/rt. Panel (e) are the Climate Prediction Center Leaky Bucket Model modeled soil moisture percentiles for January 2019.

466

Accepted for publication in *Bulletin of the American Meteorological Society.* DOI 10.1175/BAMS-D-19-0101.1.

(a)

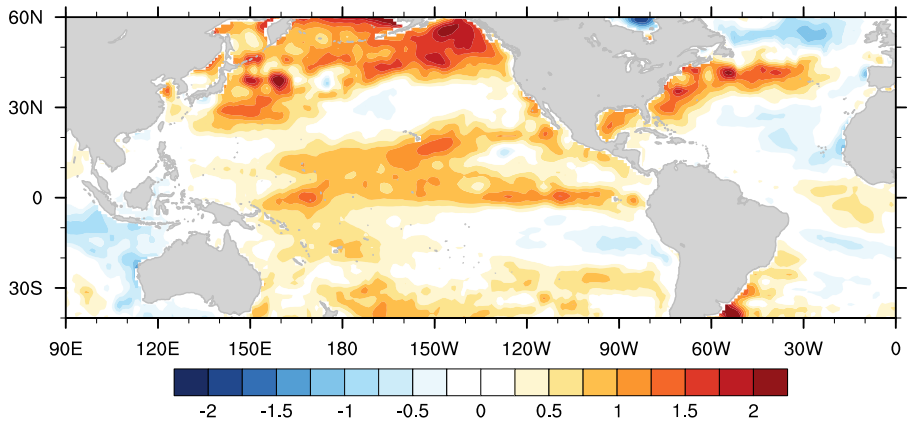

(b)

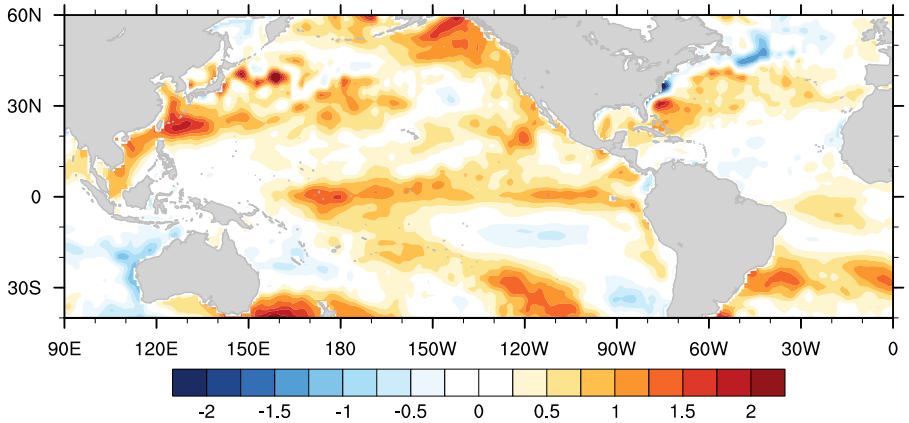

Figure 3: National Oceanic and Atmospheric Association Optimum Interpolation Sea Surface Temperature (SST) V2 anomalies for (a) September, October and November 2018 and (b) December 2018, January, and February 2019 in °C. Anomalies were calculated using the 1981-2010 base period climatology.

467

468

Accepted for publication in *Bulletin of the American Meteorological Society.* DOI 10.1175/BAMS-D-19-0101.1.

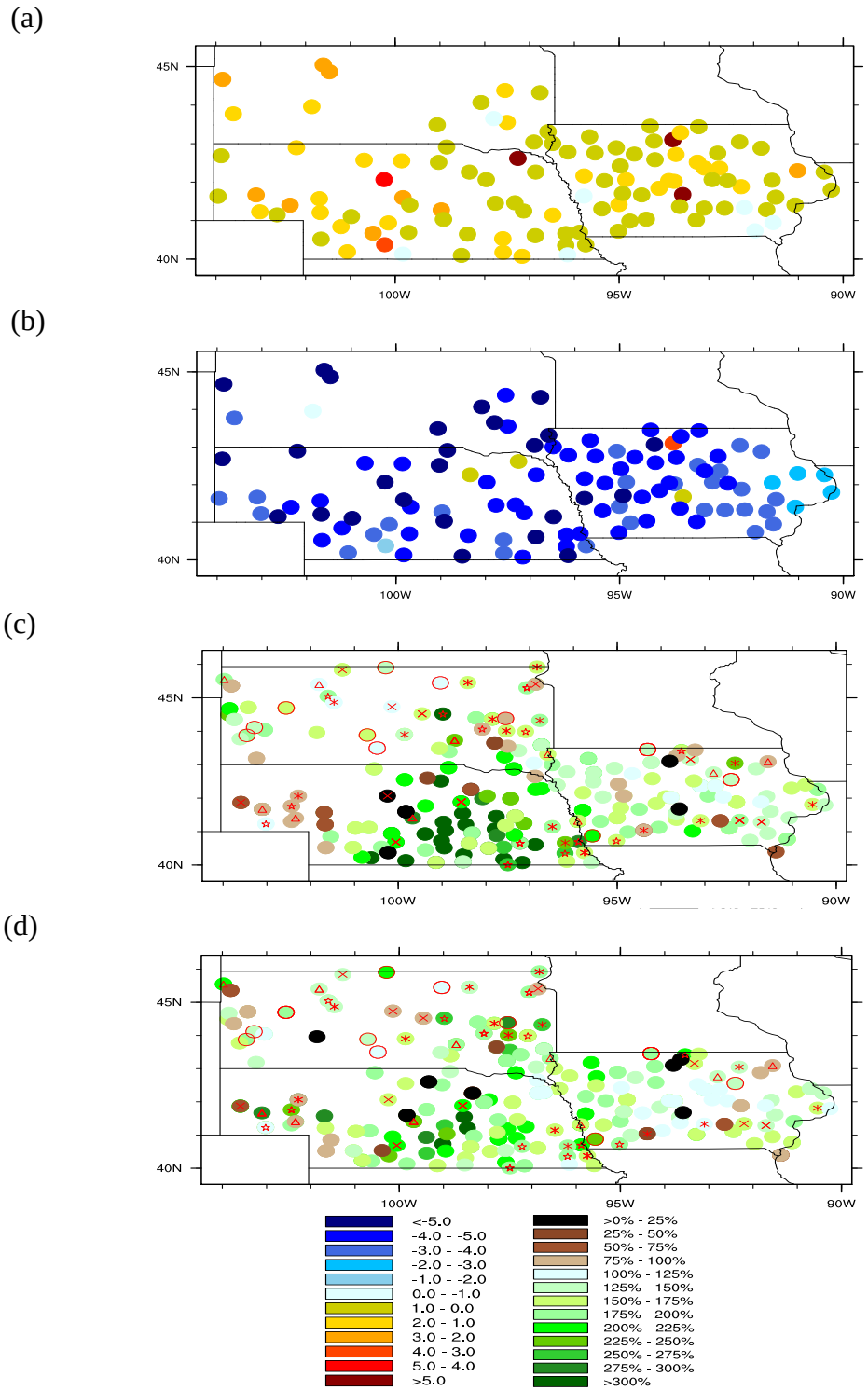

Figure 4: Global Historical Climatology Network (GHCN) station (a) monthly surface daily temperature anomalies for December and January °C, (b) monthly surface daily average temperature anomalies for February and March 2019 in °C, (c) monthly precipitation percent of normal for December 2018 and January 2019, (d) monthly precipitation percent of normal for February and March 2019. Stations were filtered by length of record, with only stations having at least 50 years of data prior to 2019

Accepted for publication in *Bulletin of the American Meteorological Society.* DOI 10.1175/BAMS-D-19-0101.1.

being accepted into the analysis. Anomalies were calculated using the period of record for each station. Daily temperature averages were computed as an average between the maximum and minimum daily temperature averages for each month. Station 2018-2019 snow season snowfall total records include a red symbol, with a circle representing a new record, a star is for a 2nd highest snowfall observation, 3 lines for a 3rd highest snowfall observation, 2 lines for a 4th highest snowfall observation, and a triangle for a 5th highest snowfall observation.

469

470

Accepted for publication in *Bulletin of the American Meteorological Society.* DOI 10.1175/BAMS-D-19-0101.1.

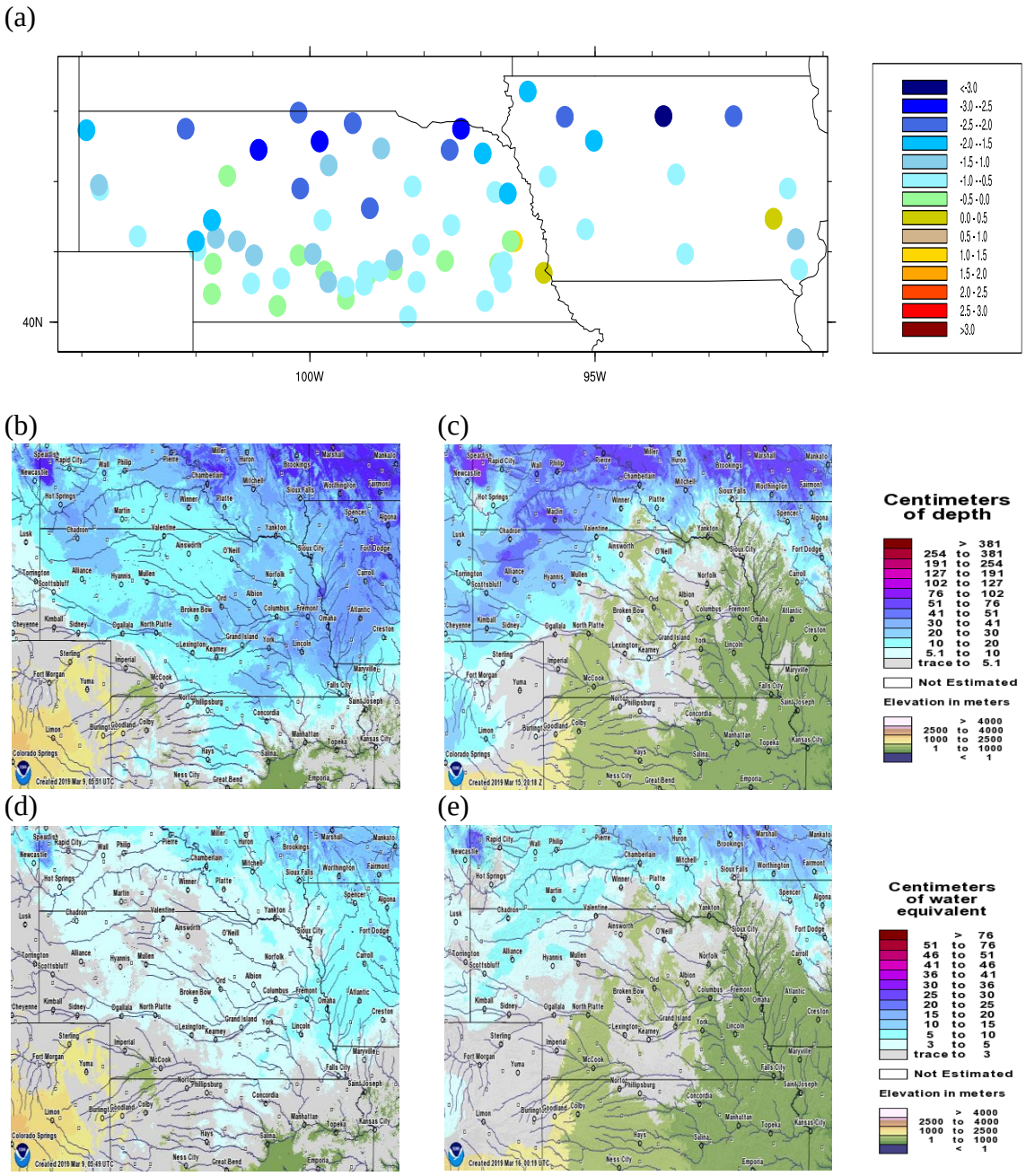

Figure 5: (a) Automated Weather Data Network (AWDN) 7-day soil temperature (°C) observations for 6 March to 12 March. National Operational Hydrologic Remote Sensing Center (NOHRSC) modeled (b) snow depth in cm for 9 March 2019 (c) 15 March and (d) snow water equivalent in cm for 9 March 2019 and (e) 15 March. Available at https://www.nohrsc.noaa.gov/.

471

472

Accepted for publication in *Bulletin of the American Meteorological Society.* DOI 10.1175/BAMS-D-19-0101.1.

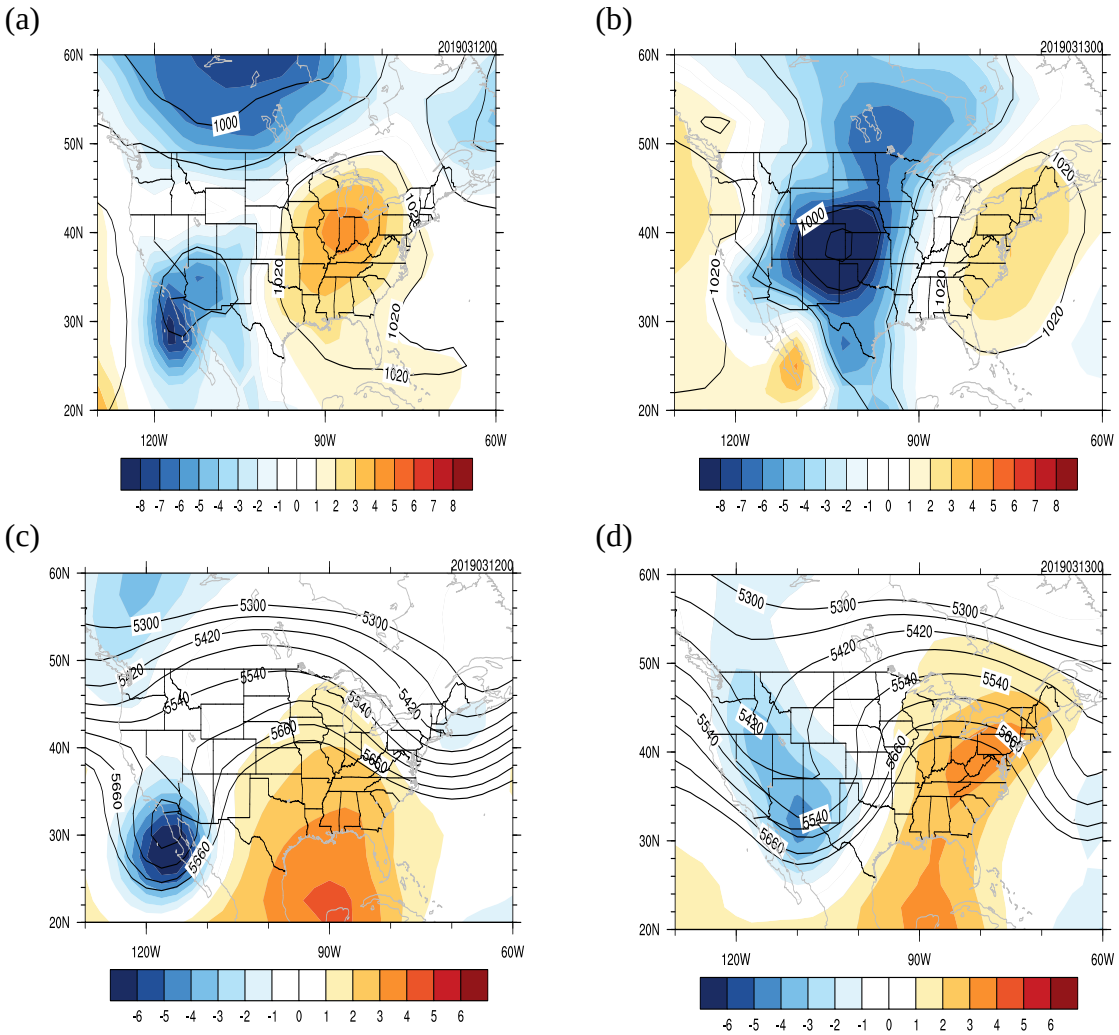

Figure 6: NCEP/NCAR Reanalysis daily averaged data for 12 March. Panel (a) is the daily averaged 500 sea level pressure (contoured) and the standardized anomaly (color filled) for March 12th. Geopotential height contours go from 900 to 1050 by 10 mb and the standardized anomalies are color filled from -8 to 8 by 1. Panel (b) is the daily averaged 500 sea level pressure (contoured) for March 13th. The contours for (b) are the same as (a). Panel (c) is the daily averaged 500 hPa geopotential height (contoured) and the standardized anomaly (color filled) for March 12th. Geopotential height contours from 5300 to 5700 with 60 m interval and the standardized anomalies are color filled from -6 to 6 by 1. Panel (d) is the daily averaged 500 hPa geopotential height (contoured) and the standardized anomaly (color filled) for March 13th. The contours for (d) are the same as (c).

473

474

Accepted for publication in *Bulletin of the American Meteorological Society.* DOI 10.1175/BAMS-D-19-0101.1.

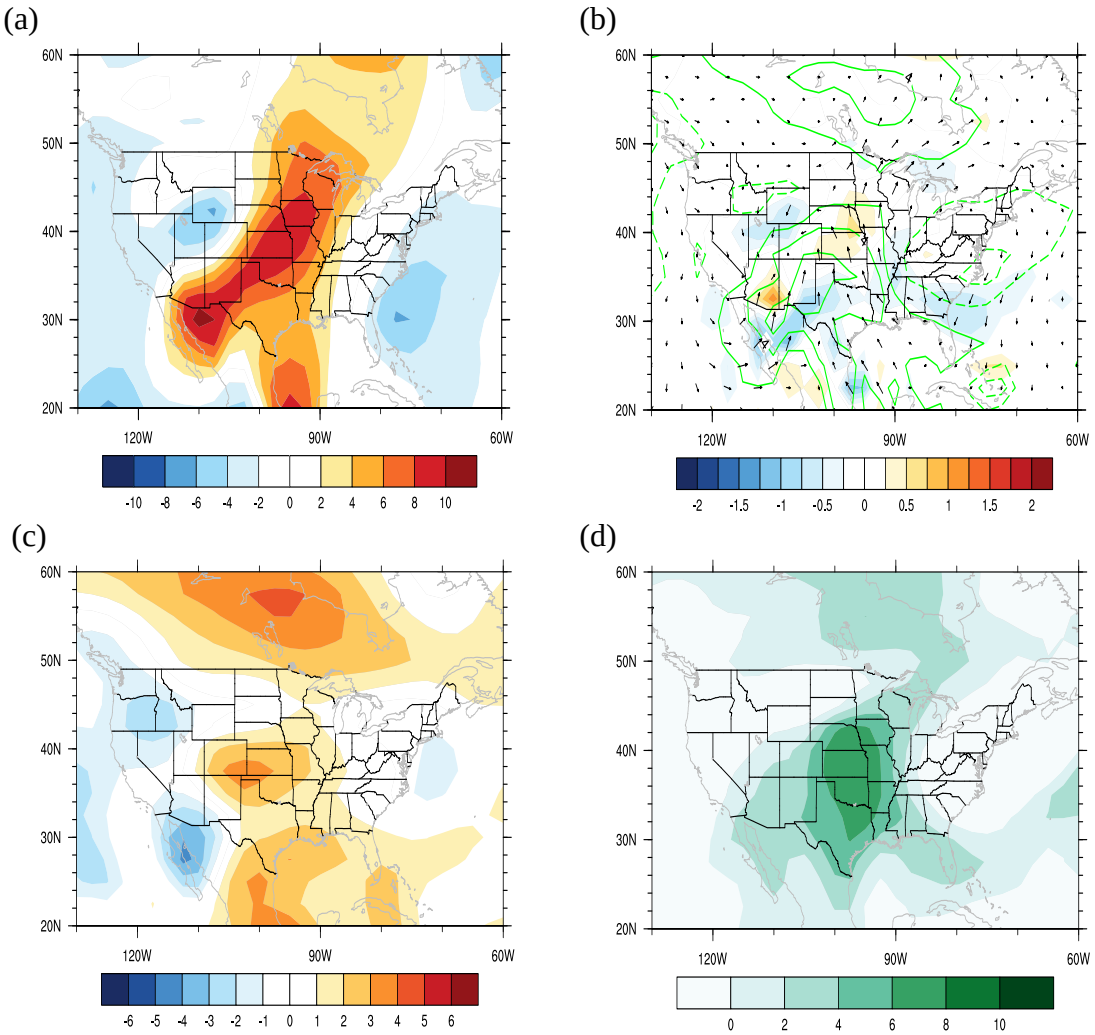

Figure 7: NCEP/NCAR Reanalysis (a) 925 mb *v* wind standardized anomalies. Panel (b) are the reanalysis 925 moisture advection standardized anomalies (g kg^{-1} s^{-1}), specific humidity standardized anomalies (g kg^{-1} contoured from -12 to 12 by 2) and standardized anomaly vector wind. Panel (c) is the surface (1000 hPa) temperature standardized anomalies (°C). Panel (d) is the precipitable water standardized anomalies (kg m^{-2}). Anomalies are from the two-day period of 12 March through 13 March 2019.

475

476

Accepted for publication in *Bulletin of the American Meteorological Society.* DOI 10.1175/BAMS-D-19-0101.1.

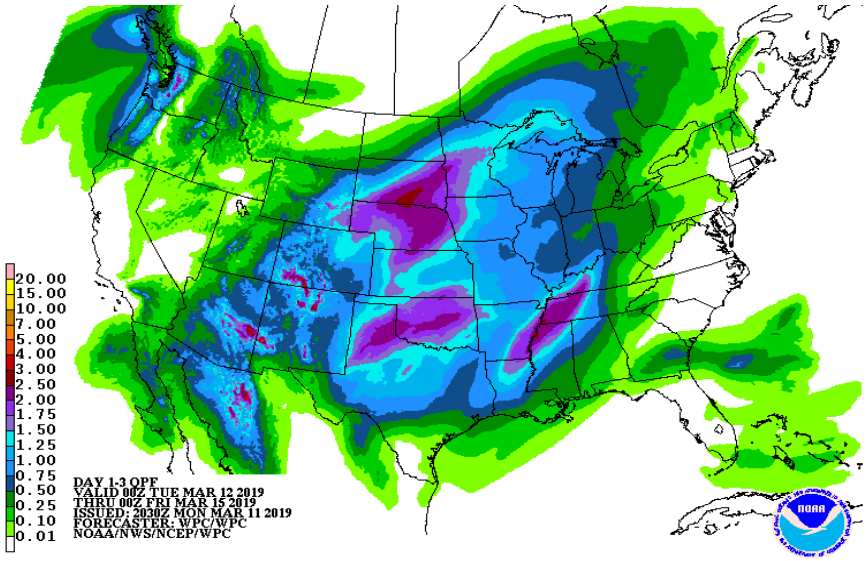

Figure 8: WPC QPF forecast made on 11 March for the 72-hour period beginning on 12 March at 0000 UTC and ending on 15 March at 0000 UTC.

477

478

Accepted for publication in *Bulletin of the American Meteorological Society.* DOI 10.1175/BAMS-D-19-0101.1.

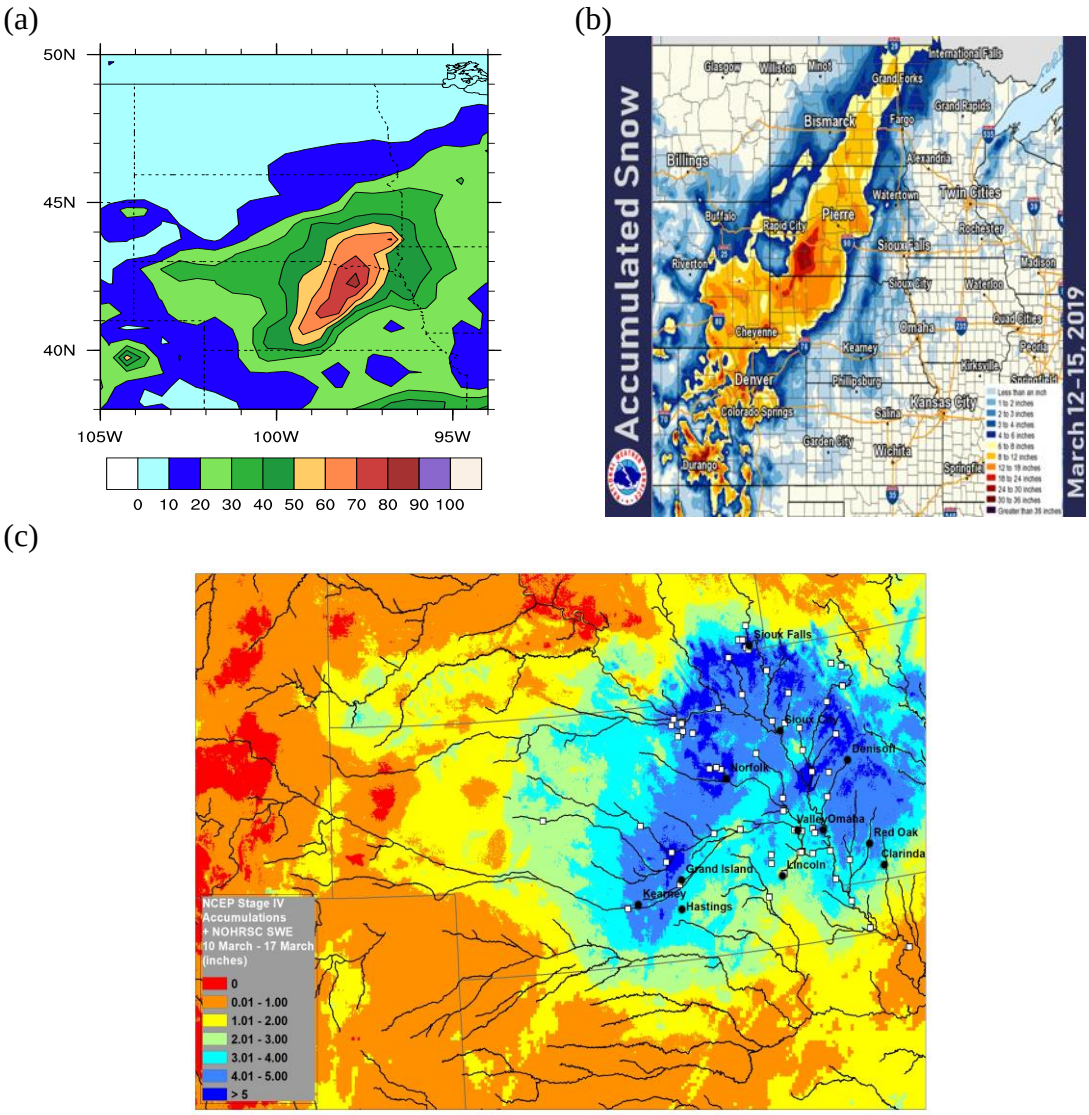

Figure 9: Panel (a) CPC Global Unified Gauge-based daily precipitation analysis for 12-14 March. Precipitation is in mm. Panel (b) is the accumulated snow for 12-15 March 2019 in inches. Available at https://www.weather.gov/fsd/20190314-Flooding. Panel (c) is the liquid precipitation and snow water equivalent totals for 10 March to 17 March 2019. The liquid precipitation totals are form the NCEP Stage IV product and the snow water equivalents are from the NOHRSC database. The white squares in (c) represent river gauges that set near flood stage records during the March flood event.

479

480

Accepted for publication in *Bulletin of the American Meteorological Society.* DOI 10.1175/BAMS-D-19-0101.1.